J Mol Model (2014) 20:2477
DOI 10.1007/s00894-014-2477-0

ORIGINAL PAPER

Hydrogen-bonded complexes between dimethyl sulfoxide and monoprotic acids: molecular properties and IR spectroscopy

Márcia K. D. L. Belarmino · Vanessa F. Cruz · Nathália B. D. Lima

Received: 30 March 2014 / Accepted: 21 September 2014 / Published online: 25 October 2014

Abstract MP2/6-31++G(d,p) and DFT B3LYP/6-31++G(d,p) calculations were performed of the structure, binding energies, and vibrational modes of complexes between dimethyl sulfoxide (DMSO) as a proton acceptor and monoprotic linear acids HX (X = F, Cl, CN) as well as monoprotic carboxylic acids HOOCR (R=–H, $–CH_3$, $–C_6H_5$) in 1:1 and 1:2 stoichiometric ratios. The results show that two different structures are possible in the 1:2 ratio: in the first, the DMSO molecule interacts with both acid molecules (leading to a "Y" structure); in the second, the DMSO interacts with only one monoprotic acid. The second structure shows a lower stability per hydrogen bond. The spontaneities of the reactions to form the 1:1 and 1:2 complexes are greatly influenced by the X group of the linear acid. With the exception of HCN, all the reactions are spontaneous. In the 1:2 complexes with Y structure, we observed that the hydrogen atoms of the linear acid are coupled in symmetric and asymmetric modes, while this type of coupling is absent from the other 1:2 complexes.

Keywords Dimethyl sulfoxide · Theoretical calculations · Hydrogen bonds · Carboxylic acid

Introduction

Hydrogen bonds in biomolecular systems are extremely important [1–7]. These interactions influence the functionalities of the molecular species, as well as our understanding of various physical properties of the system, such as energetic stabilities, structural properties, the band shift in the infrared spectrum, and chemical reactivity [8–16]. Even though the hydrogen bonds are weak in comparison with covalent bonds, they increase the stability of proteins and stabilize the structure of DNA and RNA due to interactions between the pyrimidine and purine bases [17].

A hydrogen bond forms between an electron-rich or more electronegative element (e.g., O, N, or F) and the hydrogen atom of a donor molecule. Several experimental methods are employed to characterize the existence of hydrogen bonds. Infrared (IR) and Raman spectroscopy are often performed to identify the existence of hydrogen bonds in complexes in the gas or solution phase [18, 19]. For solid-state compounds, nuclear magnetic resonance spectroscopy [5, 7, 20, 21] and X-ray diffraction [21–23] are the preferred methods. Computationally, ab initio and DFT calculations are widely used in simulations of spectroscopic properties of hydrogen-bonded complexes between a proton acceptor molecule and a proton donor molecule [8, 14, 15, 24, 25]. QTAIM theory is also employed to elucidate the electronic nature of the hydrogen bond [26, 27].

Dimethyl sulfoxide (DMSO) is an important solvent that is widely used in biomolecular systems as a drug carrier across cell membranes [19]. The partial negative charge on the oxygen atom of the DMSO molecule favors the formation of hydrogen bonds with proton donor molecules. For example, studies of complexes involving DMSO and water molecules showed nonideal behavior of the mixture [28].

In this article, we performed MP2 and DFT B3LYP calculations of the structures, binding energies, and vibrational modes of complexes between DMSO as a proton acceptor and monoprotic linear acids HX (X = F, Cl, CN) as well as monoprotic carboxylic acids HOOCR (R=–H, $–CH_3$, $–C_6H_5$). 1:1 and 1:2 complexes between DMSO and one or two acid molecules were studied.

This paper belongs to Topical Collection Brazilian Symposium of Theoretical Chemistry (SBQT2013).

M. K. D. L. Belarmino · V. F. Cruz · N. B. D. Lima (✉)
Departamento de Química Fundamental, Universidade Federal de Pernambuco (UFPE), 50740-540, Recife, PE, Brazil
e-mail: nathalia.blima@ufpe.br

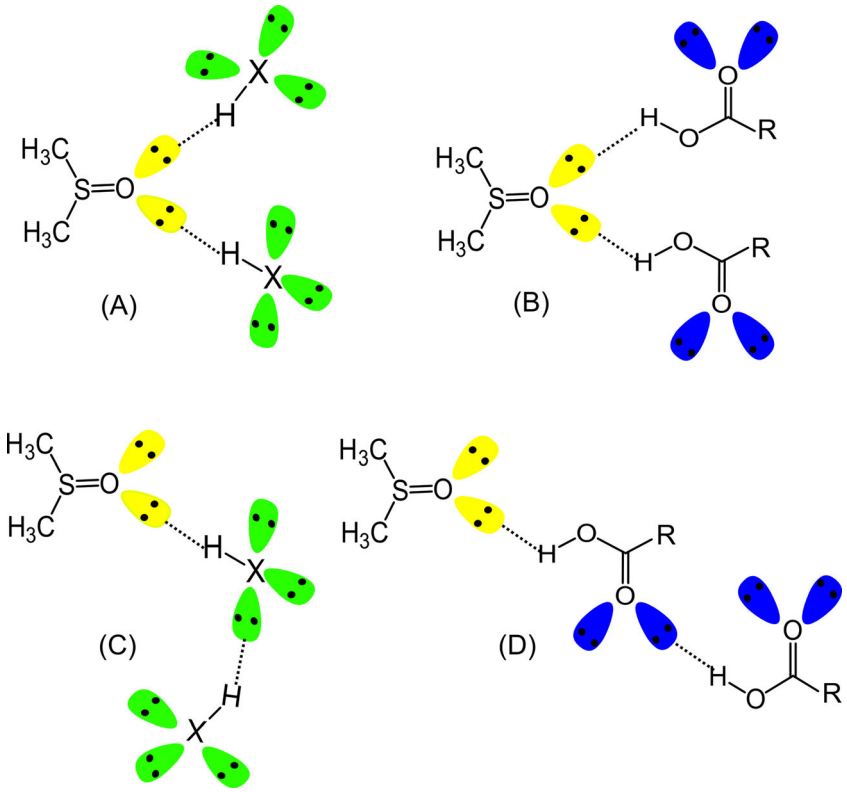

Fig. 1a–d Structures of the 1:2 complexes (X=–F, –Cl, –CN; R= –H, $–CH_3$, $–C_6H_5$): **a** DMSO···$(HX)_2$ (Y structure); **b** DMSO···$(HOOCR)_2$ (Y structure); **c** DMSO···HX···HX; **d** DMSO···HOOCR···HOOCR

Computational procedure

For comparison purposes, we performed MP2 (second-order Møller–Plesset perturbation theory) [29] and DFT B3LYP [30] calculations with the 6-31++G(d,p) basis set [31] to obtain molecular and vibrational properties of the complexes between DMSO and monoprotic acids. We optimized the geometries of the 1:1 and 1:2 hydrogen-bonded complexes. The energetic stabilities (ΔE) of the hydrogen bonds were obtained and corrected for the zero point energy (ZPE) and

Table 1 MP2/6-31++G(d,p)-derived and B3LYP/6-31++G(d,p)-derived values of structural parameters after complexation. B3LYP values are shown in parentheses

Complex	$\delta_r(X–H)_1$ (Å)	$\delta_r(X–H)_2$ (Å)	$\delta_r S=O$ (Å)
DMSO···HF	0.044 (0.048)	–	0.021 (0.023)
DMSO···HCl	0.072 (0.078)	–	0.017 (0.024)
DMSO···HCN	0.013 (0.016)	–	0.008 (0.007)
DMSO···HOOCH	0.035 (0.037)	–	0.023(0.023)
DMSO···$HOOCCH_3$	0.032 (0.033)	–	0.022(0.022)
DMSO···$HOOCC_6H_5$	0.036 (0.036)	–	0.024(0.023)
DMSO···$(HF)_2$ (Y structure)	0.026 (0.029)	0.026 (0.029)	0.038 (0.042)
DMSO···$(HCl)_2$ (Y structure)	0.026 (0.033)	0.026 (0.033)	0.027 (0.033)
DMSO···$(HCN)_2$ (Y structure)	0.011 (0.013)	0.011 (0.013)	0.020 (0.021)
DMSO···$(HOOCH)_2$ (Y structure)	0.044 (0.026)	0.044 (0.026)	0.026 (0.044)
DMSO···$(HOOCCH_3)_2$ (Y structure)	0.025 (0.024)	0.025 (0.024)	0.047 (0.041)
DMSO···$(HOOCC_6H_5)_2$ (Y structure)	0.027 (0.026)	0.027 (0.026)	0.047 (0.042)
DMSO···HF···HF	0.071 (0.081)	0.025 (0.031)	0.032 (0.035)
DMSO···HCl···HCl	0.061 (0.131)	0.012 (0.020)	0.024 (0.037)
DMSO···HCN···HCN	0.017 (0.021)	0.008 (0.010)	0.012 (0.013)
DMSO···HOOCH···HOOCH	0.044 (0.046)	0.023 (0.028)	0.025 (0.025)
DMSO···$HOOCCH_3$···$HOOCCH_3$	0.040 (0.041)	0.020 (0.024)	0.026 (0.024)
DMSO···$HOOC_6CH_5$···$HOOCC_6H_5$	0.045 (0.041)	0.020 (0.020)	0.028 (0.024)

Table 2 Uncorrected binding energies (ΔE), binding energies corrected for ZPE (ΔE^{ZPE}), binding energies after BSSE and ZPE correction ($\Delta E^{BSSE,ZPE}$), and Gibbs free energies (ΔG) of formation obtained from MP2/6-31++G(d,p) and B3LYP/6-31++G(d,p) calculations. B3LYP values are given in parentheses

Complex	ΔE (kJ mol^{-1})	ΔE^{ZPE} (kJ mol^{-1})	$\Delta E^{BSSE,ZPE}$ (kJ mol^{-1})	ΔG (kJ mol^{-1})
DMSO···HF	−65.4 (−63.7)	−55.6 (−54.2)	−54.0 (−51.2)	−22.0 (−21.0)
DMSO···HCl	−48.2 (−44.4)	−41.8 (−38.1)	−33.3 (−34.0)	−9.0 (−4.4)
DMSO···HCN	−37.7 (−33.8)	−33.0 (−30.8)	−34.6 (−26.8)	+2.1 (+5.4)
DMSO···HOOCH	−68.8 (−54.0)	−43.0 (−49.5)	−44.6 (−46.2)	−19.5 (−10.1)
DMSO···$HOOCCH_3$	−68.8 (−57.7)	−63.2 (−52.7)	−48.1 (−49.1)	−18.3 (−6.0)
DMSO···$HOOCC_6H_5$	−71.2 (−54.9)	−67.8 (−51.1)	−49.2 (−46.9)	−21.3 (−7.4)
DMSO···$(HF)_2$ (Y)	−110.0 (−104.7)	−92.0 (−87.3)	−71.6 (−80.8)	−33.7 (−27.5)
DMSO···$(HCl)_2$ (Y)	−85.7 (−70.5)	−73.0 (−58.3)	−45.4 (−50.2)	−1.3 (−0.8)
DMSO···$(HCN)_2$ (Y)	−68.9 (−56.7)	−59.7 (−48.9)	−43.6 (−46.6)	+0.4 (+9.3)
DMSO···$(HOOCH)_2$ (Y)	−117.0 (103.1)	−106.1 (−94.0)	−88.3 (−96.0)	−21.2 (−11.2)
DMSO···$(HOOCCH_3)_2$ (Y)	−126.6 (−98.0)	−116.9 (−90.1)	−86.1 (−90.5)	−32.7 (−25.5)
DMSO···$(HOOCC_6H_5)_2$ (Y)	−130.2 (−130.2)	−121.8 (−93.3)	−91.8 (−122.1)	−12.8 (−7.7)
DMSO···HF···HF	−113.9 (−113.6)	−95.9 (−96.3)	−80.9 (−107.5)	−28.9 (−30.7)
DMSO···HCl···HCl	−74.9 (−67.0)	−63.2 (−57.5)	−41.5 (−50.2)	+1.2 (+6.6)
DMSO···HCN···HCN	−68.0 (−62.7)	−58.0 (−54.2)	−48.5 (−49.3)	+1.2 (+4.0)
DMSO···HOOCH···HOOCH	−117.0 (−100.2)	−106.1 (−95.1)	−88.3 (−95.8)	−21.2 (−27.4)
DMSO···$HOOCCH_3$···$HOOCCH_3$	−114.1 (−93.0)	−105.5 (−86.0)	−85.9 (−88.4)	−24.4 (−23.3)
DMSO···$HOOC_6CH_5$···$HOOCC_6H_5$	−125.0 (−90.5)	−119.1 (−84.7)	−94.3 (−85.2)	−30.0 (−21.7)

basis set superposition error (BSSE) using the counterpoise method [32]. The vibrational modes were also calculated. Finally, the thermodynamic reaction pathways were obtained from the Gibbs free energies of the complexes in the gas phase. The calculations were performed with the Gaussian 09 program [33].

Results and discussion

Structural properties

Initially, we considered the complexes between DMSO and the monoprotic acids with a 1:1 stoichiometric ratio. A second

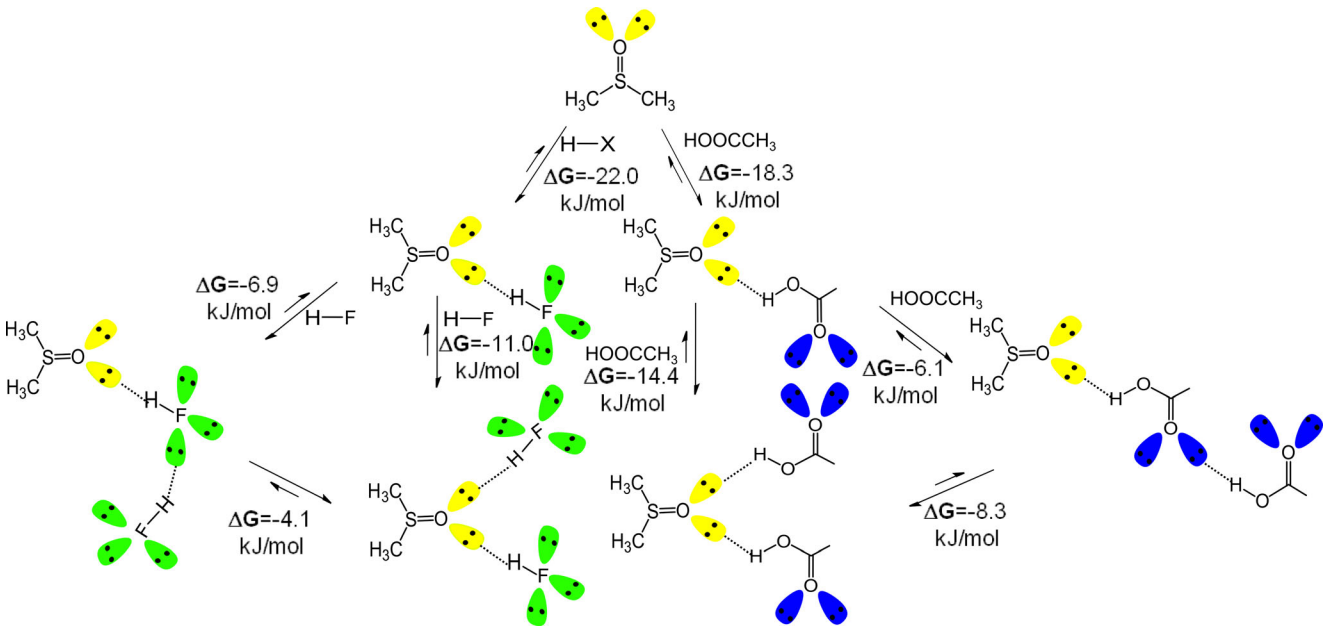

Fig. 2 Thermochemistry of the complexation reactions between DMSO and monoprotic acids (HF or $HOOCCH_3$) in stoichiometric ratios of 1:1 and 1:2

hydrogen bond was then analyzed. An angular structure was observed for the complexes DMSO···HX and DMSO···HOOCR. Two different structures were obtained for the complexes DMSO···$(HX)_2$ and DMSO···$(HOOCR)_2$. In the first, both hydrogen bonds are formed with the DMSO molecule (i.e., the complex has a "Y" structure). In the second, the monoprotic acid forms two hydrogen bonds, meaning that it acts as both a proton acceptor and a proton donor. Figure 1 illustrates the structures observed. The structures were characterized as minima because no imaginary frequencies were found. Hydrogen-bond formation usually modifies the structural properties of the molecules involved. Table 1 quantifies the structural changes observed after complexation. We observed that the bond lengths in the groups directly involved in the hydrogen bond increase. For example, in the DMSO···HOCCH complex, the H–O and S=O bond lengths (δ_r) increased by 0.035 Å and 0.023 Å, respectively. The H–X bonds of the Y-structured complexes were affected equally; for example, in the DMSO···$(HF)_2$ complex, δ_rHF and δ_rS=O were 0.026 Å and 0.038 Å, respectively.

When a second hydrogen bond is formed between the acid of the DMSO···HX complex and another acid, the acid in the middle is more strongly affected than the terminal acid. For example, in the DMSO···HF···HF complex, δ_rH–F (···H–F···) was 0.071 Å, while the length of the terminal H–F (···H–F) bond increased by only 0.025 Å.

The results indicate that these bonds are weakened by hydrogen-bond formation. This effect is probably associated with the intermolecular transfer of charge density from a lone pair on the oxygen atom to the σ* antibonding orbital of monoprotic acid [34].

Hydrogen-bond stability

Table 2 shows the MP2/6-31++G(d,p)-derived and B3LYP/6-31++G(d,p)-derived values of the uncorrected binding energies (ΔE), the binding energies after ZPE correction (ΔE^{ZPE}), the binding energies after BSSE and ZPE correction ($\Delta E^{BSSE,ZPE}$), and the Gibbs free energy of formation (ΔG) of the hydrogen

Table 3 MP2/6-31++G(d,p) and B3LYP/6-31++G(d,p) values for the harmonic frequency shifts ($\Delta\nu^{HX}$) and their intensity ratios ($A^{HX\ str,complex}/A^{HX\ str,isolated}$) in 1:1 DMSO···HX complexes. B3LYP values are given in parentheses

Complex	$\Delta\nu^{HX}$ (cm^{-1})	$A^{HX\ str,complex}/A^{HX\ str,isolated}$
DMSO···HF	−941 (−1008)	10.3 (5.5)
DMSO···HCl	−695 (−536)	6.4 (10.8)
DMSO···HCN	−197 (−217)	8.4 (10.1)
DMSO···HOOCH	−717 (−733)	25.0 (33.7)
DMSO···$HOOCCH_3$	−657 (−660)	23.5 (32.0)
DMSO···$HOOCC_6H_5$	−733 (−716)	24.8 (24.6)

Table 4 MP2/6-31++G(d,p)-derived and B3LYP/6-31++G(d,p)-derived values for harmonic frequency shifts ($\Delta\nu^{HX}$) and their corresponding intensity ratios ($A^{HX\ str,complex}/A^{HX\ str,isolated}$) in 1:2 DMSO···$(acid)_2$ complexes. B3LYP values are shown in parentheses

Complex	$\Delta\nu^{HX,sym}$ (cm^{-1})	$A^{HX,sym,complex}/A^{HX,isolated}$	$\Delta\nu^{HX,asy}$ (cm^{-1})	$A^{HX,asy,complex}/A^{isolated}$	Complex	$\Delta\nu^{HX1}$ (cm^{-1})	$A^{HX1,complex}/A^{HX,isolated}$	$\Delta\nu^{HX2}$ (cm^{-1})	$A^{HX2,complex}/A^{HX,isolated}$
DMSO···$(HF)_2$ (Y structured)	−547 (−606)	5.4 (6.8)	−590 (−656)	13.8 (16.3)	DMSO···HF···HF	−1410 (−1550)	21.7 (25.7)	−512 (−604)	6.3 (7.9)
DMSO···$(HCl)_2$ (Y structured)	−338 (−408)	28.7 (22.7)	−375 (−463)	50.2 (80.4)	DMSO···HCl···HCl	−852 (−829)	101.9 (151.2)	−161 (−385)	15.9 (45.9)
DMSO···$(HCN)_2$ Y structured)	−164 (−179)	5.2 (7.3)	−176 (−193)	8.9 (9.0)	DMSO···HCN···HCN	−251 (−141)	14.6 (6.6)	−109 (−99)	5.2 (17.5)
DMSO···$(HOOCH)_2$ (Y structured)	−470 (−494)	16.6 (10.1)	−567 (−549)	30.5 (23.5)	DMSO···HOOCH···HOOCH	−870 (−882)	30.5 (42.6)	−470 (−557)	15.7 (20.2)
DMSO···$(HOOCCH_3)_2$ (Y structured)	−482 (−462)	12.0 (18.1)	−543 (−517)	21.7 (29.7)	DMSO···$HOOCCH_3$···$HOOCCH_3$	−815 (−801)	27.3 (38.8)	−400 (−447)	17.5 (23.4)
DMSO···$(HOOCC_6H_5)_2$ (Y structured)	−512 (−495)	20.5 (22.8)	−572 (−555)	23.8 (25.9)	DMSO···$HOOC_6CH_5$···$HOOCC_6H_5$	−894 (−817)	26.6 (30.2)	−409 (−394)	16.5 (18.0)

bonds. ΔE and ΔG were determined by subtracting the sum of the total energies of the isolated molecules from the total energy of the complex.

In the 1:1 complexes between DMSO and linear monoprotic acids (HF, HCl or HCN), the order of energetic stability is HF>HCl>HCN. The MP2 $\Delta E^{BSSE,ZPE}$ values range from −33.3 kJ mol^{-1} to −54.0 kJ mol^{-1}. However, the ΔG values indicated that reaction spontaneity was greatly influenced by the X group of HX. For example, the MP2 ΔG values range from +2.1 kJ mol^{-1} to −22.0 kJ mol^{-1}.

On the other hand, for the 1:2 Y-structured complexes, the $\Delta E^{BSSE,ZPE}$ value per hydrogen bond decreased after the second complexation. For example, the MP2 $\Delta E^{BSSE,ZPE}$ value for the DMSO···HF complex is −54.0 kJ mol^{-1}, whereas this value is −71.6 kJ mol^{-1} (−35.8 kJ mol^{-1} per hydrogen bond) in the corresponding 1:2 Y-structured complex. This effect was also observed, albeit less intensely, in complexes between DMSO and monoprotic carboxylic acids. For example, the MP2 $\Delta E^{BSSE,ZPE}$ value of the DMSO···$HOOCC_6H_5$ complex is −49.2 kJ mol^{-1}, but this value is −91.8 kJ mol^{-1} (−45.9 kJ mol^{-1} per hydrogen bond) in the corresponding 1:2 Y-structured complex.

The ΔG values indicate that the second complexation is thermodynamically spontaneous for all hydrogen-bonded complexes, except in cases involving the HCN molecule; in those cases the ΔG values are always positive, whether the complex is 1:1 or 1:2.

The 1:2 complexes present similar binding energies for both structural forms. For example, the MP2 $\Delta E^{BSSE,ZPE}$ values for DMSO···$(HOOCH)_2$ (Y structured) and DMSO···HOOCH···HOOCH are almost equal. Once again, we observed that the electronegativity of the X group affects the reaction spontaneity for the complexes involving monoprotic linear acids; for systems with HF and HCN, the second hydrogen bond is probably not spontaneous. Finally, for 1:2 complexes with carboxylic acids, the second complexation is spontaneous and the R group of the HOOCR molecule does not significantly affect the stability energy and spontaneity of the complexation. The MP2 $\Delta E^{BSSE,ZPE\ range}$ values from −85.9 kJ mol^{-1} to −94.3 kJ mol^{-1}, while ΔG ranges from −21.2 kJ mol^{-1} to −30.0 kJ mol^{-1}. Figure 2 illustrates the reactions of formation of the 1:1 and 1:2 complexes between DMSO and the monoprotic acids.

Vibrational modes

In Table 3, we present the MP2/6-31++G(d,p)-derived and B3LYP/6-31++G(d,p)-derived frequency shifts observed for the H–X stretching modes and the ratios of their intensities before and after complexation for 1:1 complexes. The H–X stretching frequency of the HX monoprotic acid is shifted downwards. In both the MP2 and B3LYP calculations, the displacement ($\Delta\nu^{HX}$) is more pronounced in complexes involving the HF molecule; the MP2 $\Delta\nu$ value for the complex DMSO···HF is 941 cm^{-1}. For the 1:1 complexes between DMSO and carboxylic acids, the MP2 $\Delta\nu$ values range from −657 cm^{-1}$_{-1}$ to −733 cm^{-1}.

The infrared intensity associated with the H–X and H–O stretching modes increases upon hydrogen-bond formation. The main changes were observed for the complexes involving the carboxylic acids, where the B3LYP $A^{HOstr,complex}/A^{HOstr,isolated}$ *("str" = stretching) values range from 24.6 to 33.7.*

Two different situations occurred in the 1:2 complexes (Table 4). The first involved the Y-structured complexes, in which—due the second hydrogen bond—the hydrogen atoms of the HX stretching modes coupled to form symmetric and asymmetric vibrational modes. The second situation occurred for the DMSO···acid···acid complexes, where we observed independent vibrational modes for the HX groups. In the first situation, the harmonic frequency shifts of HX stretching in the asymmetric vibrational mode are always larger than the corresponding shifts in the symmetric mode. For example, in DMSO···$(HOOCCH_3)_2$ (Y structured), the MP2 $\Delta\nu^{HO,asy}$ and $\Delta\nu^{HO,sym}$ values are −543 cm^{-1} and −482 cm^{-1}, respectively. For the independent vibrational modes of H–X stretching, we observed that the monoprotic acid that formed two hydrogen

Table 5 MP2 and B3LYP/6-31++G(d,p) values of the harmonic frequencies ν (in cm^{-1}) and infrared intensities A (in km mol^{-1}) for the new vibrational modes that arise due to hydrogen-bond formation

New vibrational mode	Parameter	DMSO···HF	DMSO···HCl	DMSO···HCN
H-bond stretch	ν_σ (cm^{-1})	303 (296)	183 (190)	157 (146)
HX(···O)	A_σ (km mol^{-1})	14.3 (16.1)	56.1 (78.7)	27.0 (18.5)
HX $_{bend}$	$\nu_{\beta,in\text{-}plane}$ (cm^{-1})	1016 (1009)	740 (846)	912 (933)
	$A_{\beta,in\text{-}plane}$ (km mol^{-1})	441.7 (358.0)	133.5 (174.1)	77.3 (76.5)
	$\nu_{\beta,out\text{-}of\text{-}plane}$ (cm^{-1})	931 (934)	659 (744)	904 (922)
	$A_{\beta,out\text{-}of\text{-}plane}$ (km mol^{-1})	89.3 (78.5)	34.1 (38.2)	50.2 (49.0)
H $_{bend}$	$\nu_{\beta,in\text{-}plane}$ (cm^{-1})	97 (89)	66 (65)	57 (48)
	$A_{\beta,in\text{-}plane}$ (km mol^{-1})	11.8 (11.8)	3.9 (1.7)	20.7 (18.5)
	$\nu_{\beta,out\text{-}of\text{-}plane}$ (cm^{-1})	71 (61)	49 (59)	23 (29)
	$A_{\beta,out\text{-}of\text{-}plane}$ (km mol^{-1})	0.5 (0.6)	0.1 (0.1)	0.1 (0.1)

bonds (···acid···) was always the most strongly affected of the two acids. For instance, in the DMSO···$HOOCCH_3$···$HOOCCH_3$ complex, the MP2 $\Delta\nu^{\cdots HO\cdots}$ and $\Delta\nu^{\cdots HO}$ shift values are −815 cm^{-1} and −400 cm^{-1}, respectively.

Table 5 lists the frequencies of the five new vibrational modes for the 1:1 complexes between DMSO and linear monoprotic acids (HF, HCl, HCN). The new vibrational modes arise due to hydrogen-bond formation. Initially, we observed that the intermolecular stretching mode ($H_{bond\ stretch}$) that is directly associated with the hydrogen bonding ranges between 183 and 303 cm^{-1}. The IR intensity of this mode is very weak, so it is not easy to characterize this mode from the experimental vibrational spectrum. We also observed two H–X bending modes ($HX_{bending}$) that are associated with the in-plane and out-of-plane bending modes, where the proton of the HX molecule moves along a line which is perpendicular to the H−X bond axis. These two modes have considerable intensities. For the DMSO···HF complex, the MP2 IR intensities (*A*) values for the in-plane and out-of-plane bending modes of HF are 441.7 km mol^{-1} and 89.3 km mol^{-1}, respectively. Finally, we also show (in Table 5) the mode with the lowest frequency for each complex. This is associated with an intermolecular bending vibration, where the atoms of each molecule in the complex move in a direction perpendicular to the respective molecular axis. For example, its intensities for the in-plane and out-of-plane modes of the DMSO···HF complex are 11.8 km mol^{-1} and 0.5 km mol^{-1}, respectively, with frequencies of 97 cm^{-1} and 71 cm^{-1}, respectively.

Conclusions

In this work, MP2 and DFT B3LYP calculations with the 6-31++G(d,p) basis set were performed for complexes between DMSO (proton acceptor) and monoprotic linear acids HX (X = F, Cl, CN) as well as carboxylic acids HOOCR (R= –H, $–CH_3$, $–C_6H_5$) in order to obtain their structures, binding energies, and vibrational modes. Complexes with stoichiometric ratios of 1:1 and 1:2 were studied. In all cases, we observed similar behaviors for the properties whether they were calculated using MP2 or the B3LYP method. Our results show that the formation of the second hydrogen bond can result in two possible structures. In the first, DMSO behaves as a bridge; in the second, one of the acid molecules behaves as a bridge. The second complexation caused by hydrogen-bond formation leads to a decrease in the stability energy per hydrogen bond. The spontaneities of the reactions to form the 1:1 and 1:2 complexes are greatly influenced by the X group of the linear acid. With the exception of HCN, all reactions are spontaneous. In the 1:2 Y-structured complexes, we observed that the hydrogen atoms of the linear acid are coupled in symmetric and asymmetric modes, whereas this type of coupling is absent from the other 1:2 complexes.

Acknowledgments The authors gratefully acknowledge partial financial support from the Brazilian funding agencies Conselho Nacional de Desenvolvimento Científico e Tecnológico (CNPq), Programa de Apoio a Núcleos de Excelência (PRONEX), and Fundação de Amparo à Ciência e Tecnologia de Pernambuco (FACEPE). The authors also thank the Centro Nacional de Processamento de Alto Desempenho de Pernambuco (CENAPAD-PE) laboratory for providing computational resources.

References

1. Amendola V, Fabbrizzi L, Mosca L (2010) Anion recognition by hydrogen bonding: urea-based receptors. Chem Soc Rev 39:3889–3915. doi:10.1039/b822552b
2. Qi WJ, Wu D, Ling J, Huang CZ (2010) Visual and light scattering spectrometric detections of melamine with polythymine-stabilized gold nanoparticles through specific triple hydrogen-bonding recognition. Chem Commun (Camb) 46:4893–4895. doi:10.1039/c0cc00886a
3. Matray TJ, Kool ET (1998) Selective and stable DNA base pairing without hydrogen bonds. J Am Chem Soc 120:6191–6192. doi:10.1021/ja9803310
4. Betz K, Malyshev DA, Lavergne T et al (2013) Structural insights into DNA replication without hydrogen bonds. J Am Chem Soc 135:18637–18643. doi:10.1021/ja409609j
5. Nikolova EN, Gottardo FL, Al-Hashimi HM (2012) Probing transient Hoogsteen hydrogen bonds in canonical duplex DNA using NMR relaxation dispersion and single-atom substitution. J Am Chem Soc 134:3667–3670. doi:10.1021/ja2117816
6. Røhr ÅK, Hammerstad M, Andersson KK (2013) Tuning of thioredoxin redox properties by intramolecular hydrogen bonds. PLoS One 8:e69411. doi:10.1371/journal.pone.0069411
7. O'Dell WB, Baker DC, McLain SE (2012) Structural evidence for inter-residue hydrogen bonding observed for cellobiose in aqueous solution. PLoS One 7:e45311. doi:10.1371/journal.pone.0045311
8. Da Silva JBP, Silva Júnior MR, Ramos MN, Galembeck SE (2005) An ab initio study of the electronic and vibrational properties of pyrazine-HX and XH-pyrazine-HX hydrogen-bonded complexes (X=F, NC, Cl, CN and CCH). J Mol Struct 744–747:217–220. doi:10.1016/j.molstruc.2004.12.048
9. Fazli M, Raissi H, Chahkandi B, Aarabi M (2010) The effect of formation of second hydrogen bond in adjacent two-ring resonance-assisted hydrogen bonds—ab initio and QTAIM studies. J Mol Struct THEOCHEM 942:115–120. doi:10.1016/j.theochem.2009.12.009
10. Jing B, Li Q, Li R et al (2011) Competition and cooperativity between hydrogen bond and halogen bond in HNC–$(HOBr)_n$ and $(HNC)_n$–HOBr (n=1 and 2) systems. Comput Theor Chem 963:417–421. doi:10.1016/j.comptc.2010.11.006
11. Jo J, Olasz A, Chen C-H, Lee D (2013) Interdigitated hydrogen bonds: electrophile activation for covalent capture and fluorescence turn-on detection of cyanide. J Am Chem Soc 135:3620–3632. doi:10.1021/ja312313f
12. Krystkowiak E, Dobek K, Maciejewski A (2006) Origin of the strong effect of protic solvents on the emission spectra, quantum yield of fluorescence and fluorescence lifetime of 4-aminophthalimide. J Photochem Photobiol A Chem 184:250–264. doi:10.1016/j.jphotochem.2006.04.022
13. Luschtinetz R, Gemming S, Seifert G (2013) Theoretical study on the CH···NC hydrogen bond interaction in thiophene-based molecules. Comput Theor Chem 1005:45–52. doi:10.1016/j.comptc.2012.11.005

14. Yang D, Yang Y, Liu Y (2012) A TD-DFT study on the excited-state hydrogen-bonding interactions in the 2-(2-thienyl)-3-hydroxy-4(1*H*)-quinolone-$(H_2O)_3$ cluster. Comput Theor Chem 997:42–48. doi:10.1016/j.comptc.2012.07.033
15. Zabardasti A, Kakanejadifard A, Goudarziafshar H et al (2013) Theoretical study of hydrogen and halogen bond interactions of methylphosphines with hypohalous acids. Comput Theor Chem 1014:1–7. doi:10.1016/j.comptc.2013.03.008
16. Zheng P, Takayama SJ, Mauk AG, Li H (2012) Hydrogen bond strength modulates the mechanical strength of ferric-thiolate bonds in rubredoxin. J Am Chem Soc 134(9):4124–4131. doi:10.1021/ja2078812
17. Li X-Z, Walker B, Michaelides A (2011) Quantum nature of the hydrogen bond. Proc Natl Acad Sci USA 108:6369–6373. doi:10.1073/pnas.1016653108
18. Chipanina NN, Oznobikhina LP, Aksamentova TN et al (2014) Intramolecular hydrogen bond in the push–pull CF_3-aminoenones: DFT and FTIR study, NBO analysis. Tetrahedron 70:1207–1213. doi:10.1016/j.tet.2013.12.061
19. Ouyang S-L, Wu N-N et al (2010) Investigation of hydrogen bonding in neat dimethyl sulfoxide and binary mixture (dimethyl sulfoxide+ water) by concentration-dependent Raman study and *ab initio* calculation. Chin Phys B 19:123101. doi:10.1088/1674-1056/19/12/123101
20. Camacho JJ, Reyman D, Hallwass F et al (2007) Coupled hydrogen-bonding interactions between β-carboline derivatives and acetic acid. Magn Reson Chem 45(10):830–834. doi:10.1002/mrc.2049
21. Saeed A, Khurshid A, Jasinski JP et al (2014) Competing intramolecular NHOC hydrogen bonds and extended intermolecular network in 1-(4-chlorobenzoyl)-3-(2-methyl-4-oxopentan-2-yl) thiourea analyzed by experimental and theoretical methods. Chem Phys 431–432:39–46. doi:10.1016/j.chemphys.2014.01.009
22. Rivera A, Duarte Y, González-Salas D et al (2009) X-ray and hydrogen-bonding properties of 1-((1*H*-benzotriazol-1-yl)methyl)naphthalen-2-ol. Molecules 14:1234–1244. doi:10.3390/molecules14031234
23. Bryndal I, Marchewka M, Wandas M et al (2014) The role of hydrogen bonds in the crystals of 2-amino-4-methyl-5-nitropyridinium trifluoroacetate monohydrate and 4-hydroxybenzenesulfonate: X-ray and spectroscopic studies. Spectrochim Acta A 123:342–351. doi:10.1016/j.saa.2013.12.018
24. Ernsley J, Hoyte PA, Overilllb RE (1978) Ab initio calculations on the very strong hydrogen bond of the biformate anion and comparative esterification studies. J Am Chem Soc 100(11):3303–3306. doi:10.1021/ja00479a008
25. Nadvorny D et al (2011) Hydrogen bond complexes of hydantoin: a theoretical study. Int J Quan Chem 111:1436–1443. doi:10.1002/qua.22611
26. Oliveira BG (2013) Frequency shifts and interaction strength of model hydrogen-bonded systems: new NBO and QTAIM characteristics. Struct Chem 25:745–753. doi:10.1007/s11224-013-0315-0
27. De Oliveira BG (2013) Structure, energy, vibrational spectrum, and Bader's analysis of π···H hydrogen bonds and H(-δ)···H(+δ) dihydrogen bonds. Phys Chem Chem Phys 15:37–79. doi:10.1039/c2cp41749a
28. Luzara A, Chandler D (1993) Structure and hydrogen bond dynamics mixtures by computer simulations of water–dimethyl sulfoxide. J Chem Phys 98:8160. doi:10.1063/1.464521
29. Møller C, Plesset MS (1934) Note on an approximation treatment for many-electron systems. Phys Rev 46:618–622. doi:10.1103/PhysRev.46.618
30. Geerlings P, De Proft F, Langenaeker W (2003) Conceptual density functional theory. Chem Rev 103:1793–1873. doi:10.1021/cr990029p
31. Frisch MJ, Pople JA, Binkley JS (1984) Self-consistent molecular orbital methods. 25. Supplementary functions for Gaussian basis sets. J Chem Phys 80:3265
32. Boys SF, Bernardi F (1970) The calculation of small molecular interactions by the differences of separate total energies. Some procedures with reduced errors. Mol Phys 19:553–566. doi:10.1080/00268977000101561
33. Frisch MJ, Trucks GW, Schlegel HB et al. (2009) Gaussian 09, revision A.1. Gaussian, Inc., Wallingford
34. De Lima NB, Ramos MN (2012) A theoretical study of the molecular structures and vibrational spectra of the N_2O–$(HF)_2$. J Mol Struct 1008:29–34. doi:10.1016/j.molstruc.2011.11.014